

Modeling Subsurface Water Flow and Solute Transport with HYDRUS and Related Numerical Software Packages

J. Šimůnek

Department of Environmental Sciences, University of California Riverside, Riverside, CA 92521, USA

M. Th. van Genuchten

US Salinity Laboratory, USDA-ARS, 450 West Big Springs Road, Riverside, CA 92507, USA

M. Šejna

PC-Progress, Ltd., Anglická 28, 120 00 Prague, Czech Republic

ABSTRACT: HYDRUS and related software packages represent a system of numerical models for simulating variably-saturated water, heat and solute movement in the subsurface. The software packages can simulate flow and transport in one-dimensional (e.g., HYDRUS-1D, HP1, SOILCO2, and UNSATCHEM), two-dimensional (SWMS_2D, CHAIN_2D, or HYDRUS-2D), and three-dimensional (SWMS_3D or HYDRUS (2D/3D)) transport domains. While water flow in all of the models is simulated in a relatively similar manner, different solute transport modules exist in the different codes. Some models can simulate only transport of solutes independent of one another, whereas other models include biogeochemical modules simulating complex interactions between the various solutes. For example, HYDRUS-1D and UNSATCHEM models can also consider the transport of major ions and their mutual reactions, such as dissolution-precipitation, cation exchange, or aqueous complexation. The wetland module in HYDRUS (2D/3D) furthermore considers biochemical processes associated with the flow of wastewater through constructed or natural wetlands. Finally, HP1, a model resulting from coupling HYDRUS-1D and PHREEQC, accounts for a broad range of instantaneous and kinetic chemical and biological reactions, including aqueous complexation, precipitation-dissolution, cation exchange, surface complexation, and redox reactions. In this manuscript we review the various models and provide references to many of their applications.

1 INTRODUCTION

We describe in this paper a number of numerical models for simulating water flow and movement of heat and various solutes in the subsurface. The models were developed during the past 15 years or more in close collaboration between the University of California, Riverside, the U.S. Salinity Laboratory in Riverside, PC-Progress in Prague, Czech Republic, and SCK•CEN, Mol, Belgium. This manuscript serves as a companion paper to an article that will appear in the upcoming “Vadose Zone Modeling” Special Section of Vadose Zone Journal (Šimůnek et al., in press). While that article qualitatively describes the various conceptual processes forming the basis of the different programs, here we focus on the implemented mathematical models. We provide the governing equations for the various water flow, heat transport, and solute transport modules, and discuss into which HYDRUS programs they were implemented. We additionally discuss the numerical techniques used to discretize the governing flow and transport equations, and the importance of the developed graphical user interfaces to ensure wide acceptance of the software packages. We further discuss selected applications of the HYDRUS programs to demonstrate different features of the codes. Our primary focus is on the programs listed in Table 1, i.e., HYDRUS-1D, HP1, HYDRUS-2D, and HYDRUS (2D/3D).

Table 1. Synopsis of the HYDRUS suite of windows-based software packages.

Model	Ver	Dim	Brief Description	Reference
HYDRUS-1D	3.0	1D	Water flow, heat and solute transport, carbon dioxide transport, transport of major ions, major ion chemistry, transport of colloids and bacteria.	Šimůnek et al. (2005)
HP1	1.0	1D	Water flow, transport of heat and multiple components, mixed equilibrium/kinetic biogeochemical reactions.	Jacques & Šimůnek (2005)
HYDRUS-2D	2.0	2D	Water flow, heat and solute transport (discontinued, replaced with HYDRUS (2D/3D)).	Šimůnek et al. (1999)
HYDRUS (2D/3D)	1.0	2/3D	Water flow, heat and solute transport, transport of colloids and bacteria wetland module.	Šimůnek et al. (2006b), Šejna & Šimůnek (2007)

Ver – version, OS – operating system, Dim – dimensions, DOS – Disc Operating System, 1D – one-dimensional, 2D - two-dimensional and axisymmetrical three-dimensional, 3D – three-dimensional.

2 WATER FLOW

2.1 Uniform flow

Uniform variably-saturated water flow in all of these models is described using the Richards equation:

$$\frac{\partial \theta(h)}{\partial t} = \frac{\partial}{\partial x_i} \left[K(h) \left(K_{ij}^A \frac{\partial h}{\partial x_j} + K_{iz}^A \right) \right] - S(h) \quad (1)$$

where θ = volumetric water content [L^3L^{-3}]; h = pressure head [L]; K = unsaturated hydraulic conductivity [LT^{-1}]; K_{ij}^A = components of a dimensionless anisotropy tensor \mathbf{K}^A (which reduces to the unit matrix when the medium is isotropic); S = general sink/source term [$L^3L^{-3}T^{-1}$] accounting for root water uptake; t = time [T]; and x_i = spatial coordinate [L].

Because of strongly nonlinear makeup of the Richard equation, only a relatively few simplified analytical solutions can be derived. Most practical applications of (1) require a numerical solution, which can be obtained using a variety of methods such as finite differences or finite elements. Equation (1) is generally referred to as the mixed form of the Richards equation since it contains two dependent variables (i.e., the water content and the pressure head). Solutions of (1) require knowledge of two soil hydraulic functions describing the soil water retention and hydraulic conductivity properties of the porous material. The soil water retention curve (or also called the soil water characteristic curve, the capillary pressure-saturation relationship, or the pF curve) describes the relationship between the water content and the pressure head. The HYDRUS packages permit the use of analytical functions suggested by Brooks & Corey (1964), van Genuchten (1980), Kosugi (1996), and Durner (1994):

$$S_e(h) = \frac{\theta - \theta_r}{\theta_s - \theta_r} = \begin{cases} \left(\frac{h_e}{h} \right)^\lambda \\ \frac{1}{[1 + |\alpha h|^n]^m} \\ \frac{1}{2} \operatorname{erfc} \left\{ \frac{\ln(h/h_m)}{\sqrt{2}\sigma} \right\} \\ \sum_i \frac{w_i}{[1 + |\alpha_i h|^{n_i}]^{m_i}} \end{cases} \quad (2)$$

respectively, where S_e = effective saturation [-]; θ_r and θ_s = residual and saturated water contents [L^3L^{-3}], respectively; h_e = air-entry value [L]; λ = pore-size distribution index that characterizes

the width of the pore-size distribution (or the steepness of the retention function); α [L^{-1}], n [-] and $m=1/1/n$ [-] = empirical shape parameters; h_m = median pressure head [L] for which $S_e(h_m)=0.5$ and corresponding to the median pore radius; σ = standard deviation of the log-transformed soil pore radius [-] characterizing the width of the pore-size distribution; and w_i = weighting factors for the overlapping regions.

Equation (1) contains the hydraulic conductivity function which characterizes the ability of a soil to transmit water, and as such is inversely related to the resistance to water flow. Similarly as for the soil water retention curve, HYDRUS allows analytical models for the hydraulic conductivity function as suggested by Brooks & Corey (1964), van Genuchten (1980), Kosugi (1996), and Durner (1994):

$$K(S_e) = K_s \left\{ \begin{array}{l} S_e^{2/\lambda + l + 1} \\ S_e^l [1 - (1 - S_e^{1/m})^m]^2 \\ S_e^l \left\{ \frac{1}{2} \operatorname{erfc} \left[\frac{\ln(h/h_m)}{\sqrt{2}\sigma} + \sigma \right] \right\}^2 \\ \frac{(w_1 S_{e_1} + w_2 S_{e_2})^l \left(w_1 \alpha_1 [1 - (1 - S_{e_1}^{1/m_1})^{m_1}] + w_2 \alpha_2 [1 - (1 - S_{e_2}^{1/m_2})^{m_2}] \right)^2}{(w_1 \alpha_1 + w_2 \alpha_2)^2} \end{array} \right. \quad (3)$$

respectively, where K_s = saturated hydraulic conductivity [LT^{-1}]; and l = pore-connectivity parameter [-].

2.2 Nonequilibrium flow

The Richards equation (1) predicts a uniform flow process in the vadose zone, although possibly modified macroscopically by allowing the use of spatially variable soil hydraulic properties (e.g., as dictated by different soil horizons, or varying laterally). Unfortunately, the vadose zone can be extremely heterogeneous at a range of scales, from the microscopic (e.g., pore scale) to the macroscopic (e.g., field scale). Some of these heterogeneities can lead to a preferential flow process that is very difficult to capture macroscopically with the standard Richards equation. One obvious example of preferential flow is the rapid movement of water and dissolved solutes through macropores (e.g., between soil aggregates, or caused by earthworm pathways or decayed root channels) or within rock fractures, with much of the water bypassing (short-circuiting) the soil or rock matrix. However, many other causes of preferential flow exist, such as flow instabilities caused by soil textural changes or water repellency (Hendrickx & Flury 2001; Šimůnek et al. 2003), as well as lateral funneling of water due to inclined or other textural boundaries (e.g., Kung 1990).

Preferential flow in macroporous soils and fractured rocks can be described using a variety of dual-porosity or dual-permeability models (Gerke & van Genuchten 1993; Šimůnek et al. 2003). Dual-porosity and dual-permeability models both assume that the porous medium consists of two interacting pore regions, one associated with the inter-aggregate, macropore, or fracture system, and one comprising the micropores (or intra-aggregate pores) inside soil aggregates or the rock matrix. Dual-porosity models assume that water in the matrix is stagnant, while dual-permeability models allow also for water flow within the soil or rock matrix.

2.2.1 Dual-porosity model

The dual-porosity models implemented in the HYDRUS-1D and HYDRUS (2D/3D) packages assume that water flow is restricted to the macropores (or the inter-aggregate pores and fractures), and that water in the matrix (the intra-aggregate pores or the rock matrix) does not move at all. This conceptualization partitions the liquid phase into mobile (flowing, inter-aggregate), θ_{mo} , and immobile (stagnant, intra-aggregate), θ_{im} , regions [L^3L^{-3}]:

$$\theta = \theta_{mo} + \theta_{im} \quad (4)$$

The dual-porosity formulation for water flow is then based on a mixed formulation of the Richards equation (1) to describe water flow in the macropores (the preferential flow pathways) augmented with a mass balance equation to describe the moisture dynamics in the matrix as follows (Šimůnek et al. 2003):

$$\begin{aligned} \frac{\partial \theta_{mo}(h_{mo})}{\partial t} &= \frac{\partial}{\partial x_i} \left[K(h_{mo}) \left(K_{ij}^A \frac{\partial h_{mo}}{\partial x_j} + K_{iz}^A \right) \right] - S_{mo}(h_{mo}) - \Gamma_w \\ \frac{\partial \theta_{im}(h_{im})}{\partial t} &= -S_{im}(h_{im}) + \Gamma_w \end{aligned} \quad (5)$$

where h_{im} and h_{mo} = pressure heads for both regions [T^{-1}]; S_{im} and S_{mo} = sink terms for both regions [T^{-1}]; and Γ_w = transfer rate for water from the inter- to the intra-aggregate pores [T^{-1}].

Examples of applications of dual-porosity models to a range of laboratory and field data involving transient flow and solute transport are given by Šimůnek et al. (2001), Castiglione et al. (2003), Zhang et al. (2004), Köhne et al. (2004a, 2005), Kodešová et al. (2005) and Haws et al. (2005).

2.2.2 Dual-permeability model

Research versions of HYDRUS-1D and the two-dimensional computational module of HYDRUS (2D/3D) implement the dual-permeability approach suggested by Gerke & van Genuchten (1993). This approach applies Richards equations to each of two pore regions. The flow equations for the macropore or fracture (subscript f) and matrix (subscript m) pore systems in this approach are given by:

$$\begin{aligned} \frac{\partial \theta_f(h_f)}{\partial t} &= \frac{\partial}{\partial x_i} \left[K_f(h_f) \left(K_{ij}^A \frac{\partial h_f}{\partial x_j} + K_{iz}^A \right) \right] - S_f(h_f) - \frac{\Gamma_w}{w} \\ \frac{\partial \theta_m(h_m)}{\partial t} &= \frac{\partial}{\partial x_i} \left[K_m(h_m) \left(K_{ij}^A \frac{\partial h_m}{\partial x_j} + K_{iz}^A \right) \right] - S_m(h_m) + \frac{\Gamma_w}{1-w} \end{aligned} \quad (6)$$

respectively, where w = ratio of the volumes of the macropore or fracture domain and the total soil system [-]. Note that the water contents θ_f and θ_m in (1) have different meanings than in (5) where they represented water contents of the total pore space (i.e., $\theta = \theta_{mo} + \theta_{im}$), while in (6) they refer to water contents of the two separate (fracture or matrix) pore domains such that $\theta = w\theta_f + (1-w)\theta_m$.

Examples of applications of dual-permeability models to a range of laboratory and field data involving transient flow and solute transport are given by Pot et al. (2005), Kodešová et al. (2005), and Köhne et al. (2006).

2.3 Water flow and vapor transport

The Richards equation (1) considers only water flow in the liquid phase and ignores the effects of the vapor phase on the overall water mass balance. While this assumption is justified for the majority of applications, a number of problems exist in which the effect of vapor flow can not be neglected. Vapor movement is often an important part of the total water flux when the soil moisture becomes relatively low. Scanlon et al. (2003) showed that water fluxes in deep vadose zone profiles of the arid and semiarid regions of the western U.S. are often dominated by thermal vapor fluxes. Nonisothermal liquid and vapor flow in an unpublished research version of HYDRUS is described using the equation (e.g., Saito et al. 2006):

$$\frac{\partial \theta(h)}{\partial t} = \frac{\partial}{\partial x_i} \left[(K + K_{vh}) \left(K_{ij}^A \frac{\partial h}{\partial x_j} + K_{iz}^A \right) + (K_{LT} + K_{vT}) K_{ij}^A \frac{\partial T}{\partial x_j} \right] - S(h) \quad (7)$$

where θ = total volumetric water content, being the sum ($\theta = \theta_l + \theta_v$) of the volumetric liquid water content, θ_l , and the volumetric water vapor content, θ_v (both expressed as an equivalent water content), T = temperature [K]; K = isothermal hydraulic conductivity for the liquid phase [LT^{-1}]; K_{LT} = thermal hydraulic conductivity for the liquid phase [$\text{L}^2\text{K}^{-1}\text{T}^{-1}$]; K_{vh} = isothermal vapor hydraulic conductivity [LT^{-1}]; K_{vT} = thermal vapor hydraulic conductivity [$\text{L}^2\text{K}^{-1}\text{T}^{-1}$]. Overall water flow in (7) is given as the sum of isothermal liquid flow, isothermal vapor flow, gravitational liquid flow, thermal liquid flow, and thermal vapor flow. Since several terms of (7) are a function of temperature, this equation should be solved simultaneously with the heat transport equation (11) to properly account for temporal and spatial changes in soil temperature.

Examples of HYDRUS-1D applications that consider the simultaneous movement of water in the liquid and vapor phases are given by Scanlon et al. (2003) and Saito et al. (2006). Scanlon et al. (2003) evaluated response of several semiarid (High Plains, Texas) and arid (Chihuahuan Desert, Texas; Amargosa Desert, Nevada) sites to paleoclimatic forcing using water-potential and Cl profiles, and by modeling nonisothermal liquid and vapor flow and Cl transport. They used HYDRUS-1D to show that upward nonisothermal liquid and vapor flow for at least 1 to 2 kyr in the High Plains and for 12 to 16 kyr in the Chihuahuan and Amargosa desert sites is required to reproduce measured upward water potentials and Cl profiles. Saito et al. (2006) additionally combined a numerical solution of the water flow (7) and heat transport (11) equations with water and energy balances at the soil surface. Their analyses of the distributions of the liquid and vapor fluxes versus depth showed that the soil water dynamics close to the soil surface is strongly associated with the soil temperature regime.

2.4 Water flow with freezing and thawing

Although considering both liquid and vapor flow, equation (7) still neglects one phenomenon that is important in cold climatic regions, i.e., freezing and thawing. To include freezing and thawing processes, (7) needs an additional term that accounts for frozen water (e.g., Hansson et al. 2004) as follows:

$$\begin{aligned} \frac{\partial \theta(h)}{\partial t} + \frac{\rho_i}{\rho_w} \frac{\partial \theta_i(T)}{\partial t} = & \\ = \frac{\partial}{\partial x_i} \left[(K + K_{vh}) \left(K_{ij}^A \frac{\partial h}{\partial x_j} + K_{iz}^A \right) + (K_{LT} + K_{vT}) K_{ij}^A \frac{\partial T}{\partial x_j} \right] - S(h) & \quad (8) \end{aligned}$$

where θ_i = volumetric ice content [L^3L^{-3}]; ρ_i = density of ice [ML^{-3}] (931 kg m^{-3}); and ρ_w = density of liquid water [ML^{-3}] ($\sim 1000 \text{ kg m}^{-3}$). This equation is even more tightly coupled with the heat transport equation (12) through the second term on the left side, since the change in the volumetric ice content depends on temperature and can be expressed using the generalized Clapeyron equation.

2.5 Overland flow

Traditionally, surface and subsurface flow processes have been considered mostly separately, with some of the processes being severely simplified when coupled surface and subsurface flow is simulated. For example, existing surface irrigation models typically still use empirical infiltration functions such as the Philip, Kostikov, modified Kostikov, and Branch infiltration equations, rather than rigorously simulating subsurface water flow and solute transport using the Richards equation for variably-saturated flow, and advection-dispersion type equations for solute transport. To overcome this deficiency, the following overland flow equation has been incorporated in HYDRUS-2D for use in combination with the atmospheric boundary condition at the surface boundary (Šimůnek 2003):

$$\frac{\partial h}{\partial t} + \frac{\partial Q}{\partial x} = q(x, t) \quad (9)$$

$$Q = \alpha h^m \quad \text{where} \quad \alpha = \frac{S^{1/2}}{n} \quad \text{and} \quad m = 5/3$$

where h = unit storage of water (or mean depth for smooth surfaces) [L]; Q = discharge per unit width [L^2T^{-1}], x = distance coordinate over the soil surface [L]; $q(x, t)$ = rate of local input, or lateral inflow (i.e., local precipitation minus local infiltration) [LT^{-1}]; α [$L^{2-m}T^{-1}$] and m [-] = parameters related to slope, surface roughness, and the flow conditions (laminar or turbulent flow), usually evaluated using Manning's hydraulic resistance law; S = slope [-]; and n = Manning's roughness coefficient for overland flow [-].

Figure 1 shows a simple application of the overland flow module in HYDRUS-2D to simulate flow in a hillside transect in which the soil material in the middle third of the transect (between 33 and 66 m) has a 100 times higher saturated hydraulic conductivity than the remaining soil (25 versus 0.25 $m d^{-1}$). Because of this, the middle section can accommodate the infiltration of water from both the rainfall itself and from runoff from the upgradient part of the hillslope. The soil transect had a slope of 0.01, while the roughness coefficient n was assumed to be equal to 0.01.

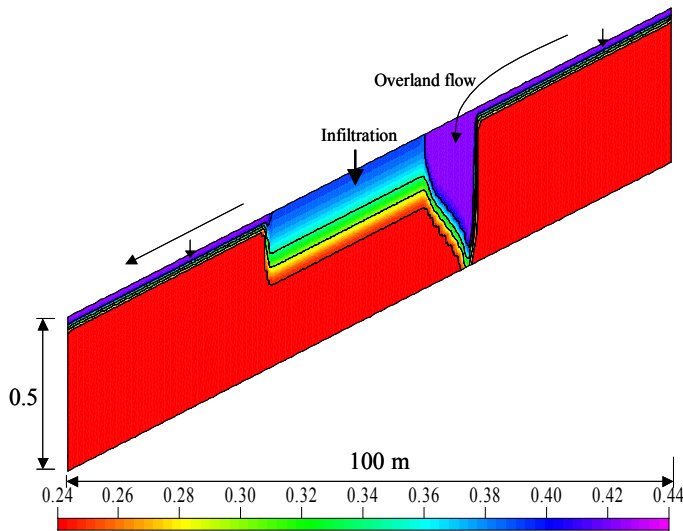


Figure 1. Calculated contours of the water content in a hillside transect following rainfall and overland flow (Šimůnek 2003).

2.6 HYDRUS package for MODFLOW

Although computer power has increased tremendously during the last few decades, large scale three-dimensional applications evaluating water flow in the vadose zone are often still prohibitively expensive in terms of computational resources. To overcome this problem, Seo et al. (2006, 2007) developed a computationally efficient one-dimensional unsaturated flow HYDRUS package and linked it to the three-dimensional modular finite-difference ground water model MODFLOW-2000 (Harbaugh et al. 2000). The HYDRUS unsaturated flow package used HYDRUS-1D to simulate one-dimensional vertical variably-saturated flow. MODFLOW zone arrays were used to define the cells to which the HYDRUS package was applied. MODFLOW used the time-averaged flux from the bottom of the unsaturated zone as recharge, and calculated a water table depth which was then used as a pressure head bottom boundary for HYDRUS. Twarakavi et al. (in press) provided a comparison of the HYDRUS package to other MODFLOW packages that evaluate processes in the vadose zone and presented a field application demonstrating the functionality of the package.

3 HEAT TRANSPORT

3.1 Heat transport without vapor transport

All HYDRUS models consider heat transport due to conduction and convection with flowing water. Neglecting the effects of water vapor diffusion, the heat transport can be described as:

$$C(\theta) \frac{\partial T}{\partial t} = \frac{\partial}{\partial x_i} \left(\lambda_{ij}(\theta) \frac{\partial T}{\partial x_j} \right) - C_w q_i \frac{\partial T}{\partial x_i} \quad (10)$$

where $\lambda_{ij}(\theta)$ = apparent thermal conductivity of the soil [$\text{MLT}^{-3}\text{K}^{-1}$] (e.g. $\text{Wm}^{-1}\text{K}^{-1}$); $C(\theta)$ and C_w = volumetric heat capacities [$\text{ML}^{-1}\text{T}^{-2}\text{K}^{-1}$] (e.g. $\text{Jm}^{-3}\text{K}^{-1}$) of the porous medium and the liquid phase, respectively; and q_i = fluid flux density [LT^{-1}]. The HYDRUS models at each time step first numerically solve the Richards equation (1) and then the heat transport equation (10) using calculated values of the water content and the fluid flux.

3.2 Heat transport with vapor transport

When the effects of water vapor diffusion can not be neglected, the heat transport must be expanded to the form (e.g., Saito et al. 2006):

$$C(\theta) \frac{\partial T}{\partial t} + L_0 \frac{\partial \theta_v}{\partial t} = \frac{\partial}{\partial x_i} \left(\lambda_{ij}(\theta) \frac{\partial T}{\partial x_j} \right) - C_w q_i \frac{\partial T}{\partial x_i} - C_v \frac{\partial q_{vi} T}{\partial x_i} - L_0 \frac{\partial q_{vi}}{\partial x_i} \quad (11)$$

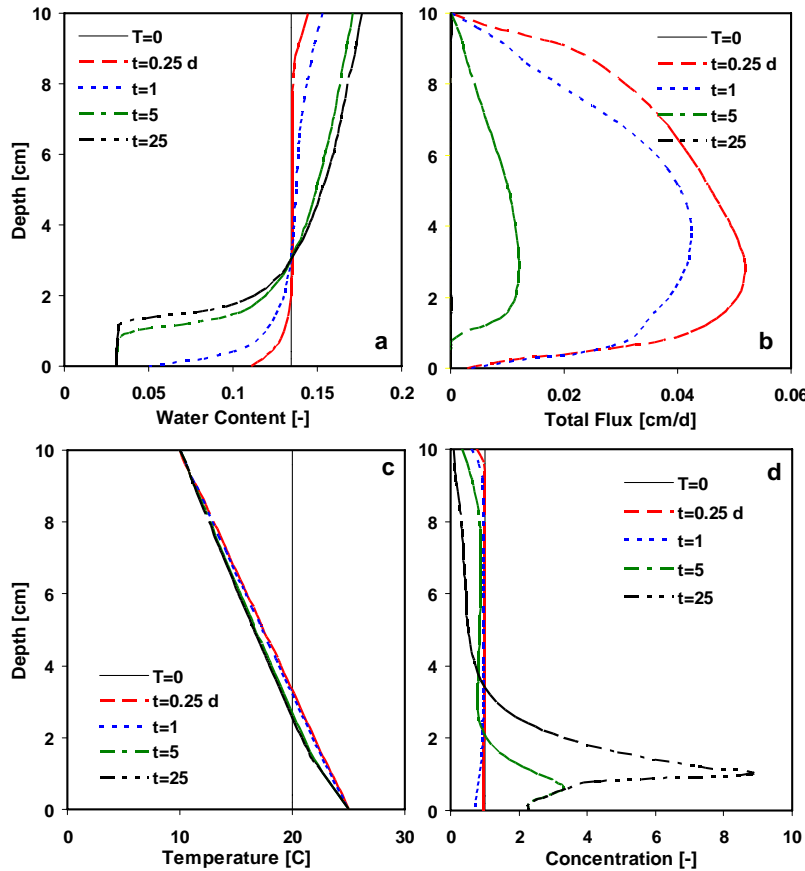


Figure 2. Water content (a), total flux (b), temperature (c), and solute concentration (d) distributions in a 10-cm long vertical soil sample with zero water fluxes across the top and bottom boundaries, and with temperature increasing from top to bottom.

where L_0 = volumetric latent heat of vaporization of liquid water [$\text{ML}^{-1}\text{T}^{-2}$] (e.g., Jm^{-3}); and q_{vi} = vapor flux density [LT^{-1}]. In equation (11), the total heat flux density is defined as the sum of the conduction of sensible heat as described by Fourier's law (the first term on the right side), sensible heat by convection of liquid water (the second term) and water vapor (the third term), and of latent heat by vapor flow (the fourth term) (de Vries 1958).

As an example, Figure 2 shows calculated water content, total flux, temperature and concentration profiles for a 10-cm long soil sample with zero water fluxes at both top and bottom boundaries, and with a temperature gradient along the sample. Increasing temperatures (Fig. 2c) from the top to the bottom of the sample cause vapor flow (Fig. 2b) from the warmer bottom end of the sample toward the colder end. Water evaporates at the warmer end, flows upward as vapor and condensates at the colder end. Water contents correspondingly decrease at the warmer end and increase at the colder bottom (Fig. 2a). As a consequence of changing water contents, a pressure head gradient develops in the sample, leading to water flow in a direction opposite to vapor flow. A steady-state is eventually reached when the upward vapor flow fully balances the downward liquid flow (Fig. 2b). Since water evaporates at the bottom of the sample and condensates at the top, solute becomes more concentrated near the bottom and more diluted near the top (Fig. 2d). Also, the concentration profile should eventually reach steady-state, although at a much larger time, when the advective downward solute flux balances the upward diffusive flux.

3.3 Heat transport with freezing and thawing

Similar to water flow, considering freezing and thawing in the heat transport equation requires an additional term to account for the energy stored in the frozen water (e.g., Hansson et al. 2004):

$$\begin{aligned} C(\theta) \frac{\partial T}{\partial t} - L_f \rho_i \frac{\partial \theta_i}{\partial t} + L_0 \frac{\partial \theta_v}{\partial t} = \\ = \frac{\partial}{\partial x_i} \left(\lambda_{ij}(\theta) \frac{\partial T}{\partial x_j} \right) - C_w q_i \frac{\partial T}{\partial x_i} - C_v \frac{\partial q_{vi} T}{\partial x_i} - L_0 \frac{\partial q_{vi}}{\partial x_i} \end{aligned} \quad (12)$$

where L_f = latent heat of freezing [L^2T^{-2}] ($\sim 3.34\text{e}+5 \text{ J kg}^{-1}$). The first term on the left-hand side represents changes in the energy content, whereas the second and third terms represent changes in the latent heat of the frozen and vapor phases, respectively. Terms on the right-hand side represent respectively, soil heat flow by conduction, convection of sensible heat with flowing water, transfer of sensible heat by diffusion of water vapor, and transfer of latent heat by diffusion of water vapor. Hansson et al. (2004) discussed the extreme nonlinearity of (12) caused by the dependency of the apparent volumetric heat capacity ($= C - L_f \rho_i d\theta_i / dT$) on temperature. While the apparent heat capacity increases by about two orders of magnitude for silty clay when the freezing point is reached, the increase for sand is almost five orders of magnitude (Fig. 3). For sands the increase in the apparent heat capacity due to freezing becomes negligible below about -0.05°C , which corresponds to a pressure head of -6.2 m . At that temperature almost all soil water is frozen, except for the residual water content. For fine-textured soils the increase in the apparent heat capacity extends to much lower temperatures, which reflects the fact that for these soils a significant amount of water remains unfrozen at slightly subzero temperatures.

Hansson et al. (2004) used HYDRUS-1D to evaluate data from laboratory column freezing experiments. The experiments involved 20-cm long soil columns with an internal diameter of 8 cm that were exposed at the top to a circulating fluid with a temperature of -6°C . Water and soil in the columns froze from the top down during the experiment, with the freezing process inducing significant water redistribution within the soil. Values of the total water content calculated with HYDRUS-1D compared well with measured values.

Figure 4 shows temperatures, pressure heads, liquid water contents, and concentrations at different depths in a loamy soil profile subject to fluctuating surface temperatures. Surface temperatures followed the sinusoidal curve with a mean value of -1°C and a daily amplitude of 5°C . Changes in temperature can be observed down to a depth of about 10 cm (Fig. 4a). The Clapeyron equation predicts that a temperature decrease of 1°C below zero corresponds to a pressure head decrease of about -120 m . This shows that negative temperatures can cause extremely

negative pressure heads in the soil profile (Fig. 4b). These pressure heads have their corresponding water contents (Fig. 4c), which follow immediately from the soil water retention curve. The remaining water within the soil profile stays in a frozen state. From Figure 4 it is obvious that the process of freezing is very similar to drying, with frozen water remaining in the larger pores and liquid water in the smaller pores. Concentrations fluctuate in a similar fashion as the other variables since solutes are excluded from frozen water and remain in the liquid phase (Fig. 4d).

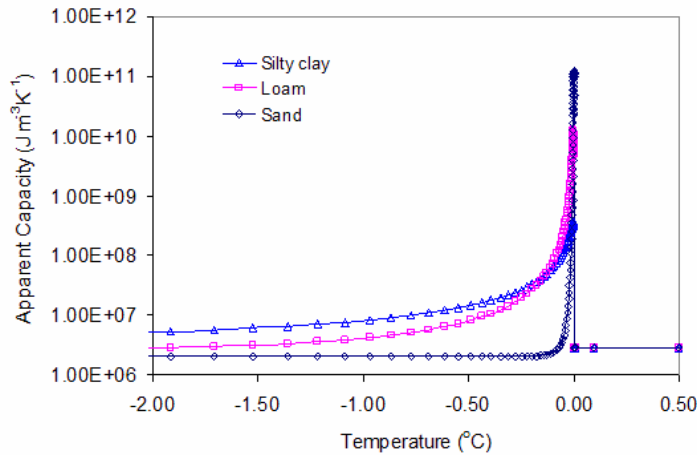


Figure 3. Apparent volumetric heat capacity ($\text{Jm}^{-3}\text{K}^{-1}$) for three soil textural classes (sand, loam, and silty clay).

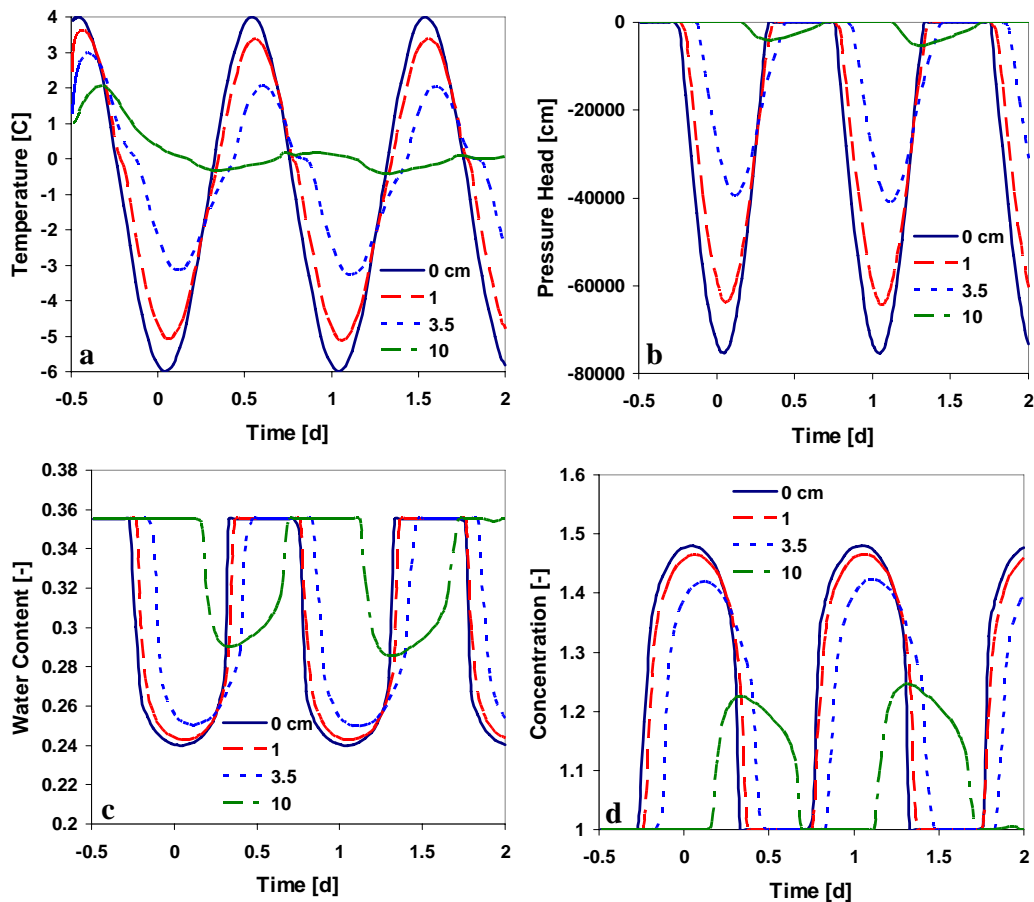


Figure 4. Temperatures (a), pressure heads (b), water contents (c), and concentrations (d) at different depths in a loamy soil profile subject to fluctuating surface temperatures.

4 SOLUTE TRANSPORT

While water flow in the various HYDRUS software packages is simulated in a relatively similar manner (i.e., using the Richards equation to describe uniform flow, or using dual-porosity or dual-permeability models for nonequilibrium flow), different solute transport modules exist in the different codes. Some modules simulate single-component transport, while others contain biogeochemical modules for simulating potentially very complex interactions between the various solutes. In this section we provide brief descriptions of the various solute transport modules.

4.1 Single component solute transport

Most HYDRUS predecessors (e.g., SWMS_2D and SWMS_3D) allowed solutes to exist only in the liquid and solid phases. The newer windows-based HYDRUS models (i.e., HYDRUS-1D, HYDRUS-2D and HYDRUS (2D/3D)) assume that solutes can exist in all three phases (liquid, solid, and gaseous) and that the decay and production processes can be different in each phase. While in the HYDRUS predecessors solutes could be transported only by advection and dispersion in the liquid phase, the more recent versions assume that they can be transported also by diffusion in the gas phase. In the various solute transport formulations below we will use the following general conservation equation for solutes in a variably saturated rigid porous medium

$$\frac{\partial M}{\partial t} = -\frac{\partial J_{Si}}{\partial x_i} - \phi \quad (13)$$

where M = mass of solute [ML^{-3}]; J_{Si} = solute flux density [$\text{ML}^{-2}\text{T}^{-1}$]; and ϕ = coefficient representing various sinks and sources [$\text{ML}^{-3}\text{T}^{-1}$].

4.1.1 Equilibrium transport

The SWMS_2D and SWMS_3D models (Šimůnek et al. 1994, 1995) assume that solutes reside only in the liquid and solid phases. The various terms of (13) are then given by:

$$\begin{aligned} M &= \theta c + \rho s \\ J_{Si} &= -\theta D_{ij}^w \frac{\partial c}{\partial x_j} + q_i c \\ \phi &= -\mu_w \theta c - \mu_s \rho s + \gamma_w \theta + \gamma_s \rho - S c_r \end{aligned} \quad (14)$$

where c , s = solute concentrations in the liquid [ML^{-3}] and solid [MM^{-1}] phases, respectively; μ_w , μ_s = first-order rate constants for solutes in the liquid and solid phases [T^{-1}], respectively; γ_w , γ_s = zero-order rate constants for the liquid [$\text{ML}^{-3}\text{T}^{-1}$] and solid [T^{-1}] phases, respectively; ρ = soil bulk density [ML^{-3}]; S = sink term in the water flow equation (1); c_r = concentration of the sink term [ML^{-3}]; D_{ij}^w = dispersion coefficient tensor [L^2T^{-1}] for the liquid phase.

The HYDRUS models allow solutes to exist also in the gaseous phase, as well as permit them to be involved in sequential first-order decay chain reactions. The different terms of (13) then become:

$$\begin{aligned} M_k &= \theta c_k + \rho s_k + a_v g_k & k = 1, N_s \\ J_{Si,k} &= -\theta D_{ij,k}^w \frac{\partial c_k}{\partial x_j} - a_v D_{ij,k}^g \frac{\partial g_k}{\partial x_j} + q_i c_k \\ \phi_k &= -(\mu_{w,k} + \mu'_{w,k}) \theta c_k - (\mu_{s,k} + \mu'_{s,k}) \rho s_k - (\mu_{g,k} + \mu'_{g,k}) a_v g_k - S c_{r,k} + \\ &\quad + \mathcal{G}(\mu'_{w,k-1} \theta c_{k-1} + \mu'_{s,k-1} \rho s_{k-1} + \mu'_{g,k-1} a_v g_{k-1}) + \gamma_{w,k} \theta + \gamma_{s,k} \rho + \gamma_{g,k} a_v \end{aligned} \quad (15)$$

where g = solute concentration in the gaseous phase [ML^{-3}]; μ_g = first-order rate constant for solutes in the gas phase [T^{-1}]; μ_w' , μ_s' , and μ_g' = similar first-order rate constants providing con-

nections between individual species in the decay chain; γ_g = zero-order rate constant for the gas phase [$\text{ML}^{-3}\text{T}^{-1}$]; a_v = air content [L^3L^{-3}]; D_{ij}^g = diffusion coefficient tensor [L^2T^{-1}] for the gas phase; and N_s = number of solutes involved in the chain reaction. The subscripts w , s , and g correspond with the liquid, solid and gas phases, respectively; while the subscript k represents the k th chain number. The parameter \mathcal{G} in (15) is zero for $k=1$. The indicial notation used above assumes summations over indices i and j ($i, j = 1, 2, 3$), but not over index k .

Interactions between the solid and liquid phases in the HYDRUS models may be described using nonlinear equations, while interactions between the liquid and gaseous phases are assumed to be linear and instantaneous, i.e.,

$$s = \frac{K_d c^\beta}{1 + \eta c^\beta} \quad (16)$$

$$g = k_g c \quad (17)$$

respectively, where K_d , β , η , k_g = empirical coefficients [L^3M^{-1}], [-], [L^3M^{-1}], [-], respectively. The Freundlich, Langmuir, and linear adsorption equations are special cases of equation (16). When $\beta=1$, equation (16) reduced to the Langmuir equation, when $\eta=0$ the equation becomes a Freundlich isotherm, and when $\beta=1$ and $\eta=0$, equation (16) defines a linear adsorption isotherm. Solute transport without adsorption is described with $K_d=0$. We note here that the SWMS_2D and SWMS_3D models considered only linear sorption (i.e., $\beta=1$ and $\eta=0$).

Typical examples of HYDRUS applications involving sequential first-order decay chains are the transport of nitrogen species (e.g., Hanson et al. 2006), pesticides, chlorinated aliphatic hydrocarbons (Schaerlaekens et al. 1999; Casey & Šimůnek 2001), hormones (Casey et al. 2003), and explosives (Dontsova et al. 2006). The ability of HYDRUS to account for diffusion in the gas phase was further used by Wang et al. (1997, 2000) to simulated the transport of volatile contaminants (fumigants) such as methyl bromine and 1,3-dichloropropene.

4.1.2 Nonequilibrium transport

HYDRUS-1D and the two-dimensional module of HYDRUS (2D/3D) offer a large number of options to deal with nonequilibrium flow and transport. A complete list of these options is given by Šimůnek et al. (in press) who divided them into three groups: a) physical nonequilibrium transport models, b) chemical nonequilibrium transport models, and c) physical and chemical nonequilibrium transport models. Physical nonequilibrium models include 1) the Mobile-Immobile Water Model, 2) the Dual-Porosity Model, 3) the Dual-Permeability Model, and 4) the Dual-Permeability Models with Immobile Water. Chemical nonequilibrium models include 1) the One Kinetic Site Model, 2) the Two-Site Model, and 3) the Two-Kinetic Sites Model. Finally, physical and chemical nonequilibrium transport models include 1) the Dual-Porosity Model with one Kinetic Site, and 2) the Dual-Permeability Model with Two-Site Sorption.

An example of **physical nonequilibrium** transport as implemented in HYDRUS is the Mobile-Immobile Water Model that uses the concept of two-region, dual-porosity type solute transport (van Genuchten & Wierenga 1976). Solute exchange between the two liquid regions is then modeled as a first-order process:

$$\frac{\partial \theta_{im} c_{im}}{\partial t} + (1 - f_{mo}) \rho \frac{\partial s_{im}}{\partial t} = \Gamma_s - \phi_{im} \quad (18)$$

$$\Gamma_s = \alpha (c_{mo} - c_{im}) + \Gamma_w c^*$$

where c_{mo} and c_{im} = concentrations of the mobile and immobile regions [ML^{-3}], respectively; s_{im} = sorbed concentration of the the immobile region [-]; ϕ_{im} = sink/source term that accounts for various zero- and first-order or other reactions in immobile region [$\text{ML}^{-3}\text{T}^{-1}$]; f_{mo} = fraction of sorption sites in contact with the mobile water content [-]; α = mass transfer coefficient [T^{-1}]; and Γ_s = mass transfer term for solutes between the mobile and immobile regions [$\text{ML}^{-3}\text{T}^{-1}$]. The first equation of (18) is a mass balance for the immobile (micropore) domain, while the second equation (Γ_s) describes the rate of mass transfer between the mobile and immobile domains. The second (advective) term of Γ_s in Eq. (18) is equal to zero for the Mobile-Immobile Model since that model does not consider water flow between the two regions. In the Dual-Porosity

Model, c^* is equal to c_{mo} for $\Gamma_w > 0$ and c_{im} for $\Gamma_w < 0$. Note that although the HYDRUS models do consider diffusive transport in the gas phase also for nonequilibrium applications, for simplicity we did not include this process in (18) and subsequent equations.

Still much more sophisticated models for physical nonequilibrium transport may be formulated. For example, Pot et al. (2005), Köhne et al. (2006), and Šimůnek et al. (in press) considered not only a dual-permeability model with flow and transport in both regions, but also a dual-permeability model that additionally divides the matrix domain into mobile and immobile subregions. Pot et al. (2005) and Köhne et al. (2006) used the HYDRUS-1D model with these dual-permeability submodels to successfully simulate bromide transport in laboratory soil columns at different flow rates or for transient flow conditions, respectively.

An example of **chemical nonequilibrium** transport in HYDRUS is the Two-Site Model that assumes that the sorption sites can be divided into two fractions:

$$s = s^e + s^k \quad (19)$$

where sorption, s^e [MM⁻¹], on one fraction of the sites (often referred to as type-1 sites) is assumed to be instantaneous, while sorption, s^k [MM⁻¹], on the remaining (type-2) sites is considered to be time-dependent. Sorption on the type-2 nonequilibrium sites is assumed to be a first-order kinetic rate process:

$$\rho \frac{\partial s^k}{\partial t} = \alpha_k \rho [s_e^k - s^k] - \phi_k \quad (20)$$

where α_k = first-order rate constant describing the kinetics of the sorption process [T⁻¹]; s_e^k = sorbed concentration that would be reached at equilibrium with the liquid phase concentration [MM⁻¹]; ϕ_k = sink/source term that accounts for various zero- and first-order or other reactions at the kinetic sorption sites [ML⁻³T⁻¹].

Although we listed the Two-Kinetic Sites Model above among the chemical nonequilibrium models, this model could equally well be viewed as a **physical and chemical nonequilibrium** transport model. This because both physical and chemical nonequilibrium processes could be responsible for solutes associated with each of the two sites. For example, while the chemical process of attachment/detachment could be associated with one fraction of sorption sites, the physical process of straining could be associated with the second fraction of sorption sites. In the Two-Kinetic Sites Model the sorption sites are again divided into two fractions:

$$s = s_1^k + s_2^k \quad (21)$$

but now both sorption sites are assumed to be kinetic. In (21), s_1^k and s_2^k = concentrations of the first and second fraction of kinetic sorption sites [MM⁻¹], respectively. The kinetic processes are then described as follows:

$$\begin{aligned} \rho \frac{\partial s_1^k}{\partial t} &= k_{a1} \theta c - k_{d1} \rho s_1^k - \phi_{k1} \\ \rho \frac{\partial s_2^k}{\partial t} &= k_{a2} \theta c - k_{d2} \rho s_2^k - \phi_{k2} \end{aligned} \quad (22)$$

where k_{a1} , k_{a2} = attachment coefficients for the first and second fraction of kinetic sorption sites [T⁻¹], respectively; k_{d1} , k_{d2} = detachment coefficients for the first and second fraction of kinetic sorption sites [T⁻¹], respectively; and ϕ_{k1} , ϕ_{k2} = sink/source terms for the first and second fraction of kinetic sorption sites [T⁻¹], respectively. As mentioned above, the two kinetic sites may be used to describe different processes. While the first kinetic process could be used for chemical attachment, the second kinetic process could represent physical straining of colloids or pathogenic microorganisms (e.g., Bradford et al. 2004, 2007; Gargiulo et al. 2007). Note that in (22) we do not give the nonlinear blocking coefficients to account for, for example, Langmuirian blocking to attachment or depth-dependent straining that are considered in the HYDRUS models (e.g., Bradford et al. 2004).

Details about the remaining nonequilibrium models, as well as of various applications, can be found in the HYDRUS manuals as well as in Šimůnek et al. (in press).

4.2 Multicomponent Solute Transport

The transport of reactive contaminants in the subsurface is generally affected by a large number of nonlinear and often interactive physical, chemical and biological processes. Proper simulating these processes requires a reactive transport code that couples the physical processes of water flow and advective-dispersive transport with a range of biogeochemical processes. The soil solution is always a mixture of many ions which may be involved in mutually dependent chemical processes, such as complexation reactions, cation exchange, precipitation-dissolution, sorption-desorption, volatilization, redox reactions, and degradation (Šimůnek & Valocchi 2002; Appelo & Postma 2005). The transport and transformation of many contaminants is further mediated by subsurface aerobic or anaerobic bacteria. Bacteria for example can catalyze redox reactions in which organic compounds (e.g., chlorinated hydrocarbons) act as the electron donor and inorganic substances (oxygen, nitrate, sulfate, or metal oxides) as the electron acceptor.

To be able to evaluate these type of systems, several different multicomponent modules were developed for the HYDRUS models. In addition to the single component solute transport module described above, HYDRUS-1D also includes the UNSATCHEM module (Šimůnek & Suarez 1993, 1994) that considers the transport of major ions, and their mutual reactions, such as dissolution-precipitation, cation exchange, or aqueous complexation. HYDRUS-1D has also been coupled with PHREEQC, resulting in the HP1 model (Jacques & Šimůnek 2005; Jacques et al. 2006) that accounts for a wide range of instantaneous and kinetic chemical and biological reactions, including aqueous complexation, precipitation-dissolution, cation exchange, surface complexation, and redox reactions. Finally, the CW2D wetland module (Langergraber & Šimůnek 2005, 2006) in HYDRUS (2D/3D) considers biochemical processes associated with the flow of wastewater through constructed or natural wetlands. Below we briefly review these models and indicate some of their applications.

Šimůnek & Valocchi (2002) divided geochemical transport models into two major groups: those with specific chemistry and more general models. Models with specific chemistry are generally restricted to certain prescribed chemical systems and thus are usually constrained to specific applications. The major ion chemistry UNSATCHEM module in the HYDRUS-1D software package and the CW2D wetland module in HYDRUS (2D/3D) are typical examples of models with specific chemistry. On the other hand, models with generalized chemistry provide users with much more freedom in simulating chemical systems, and thus permit a much broader range of applications. Users then either can select species and reactions from large geochemical databases, or are able to define their own species with particular chemical properties and reactions. The HP1 model represents a typical example of a model with generalized chemistry.

4.2.1 Major ion chemistry

As an alternative to the single-component approach, a major ion chemistry module based on the UNSATCHEM model (Šimůnek & Suarez 1993, 1994) was incorporated in HYDRUS-1D. This module considers the transport of major ions and carbon dioxide in soils. CO₂ transport is assumed to be governed by diffusion in both the liquid and gas phases, by advection in the liquid phase, and by respiration by both soil microorganisms and plant roots (Šimůnek & Suarez 1993):

$$\frac{\partial(c_a a_v + c_w \theta)}{\partial t} = \frac{\partial}{\partial z} \left(a_v D_a \frac{\partial c_a}{\partial z} \right) + \frac{\partial}{\partial z} \left(\theta D_w \frac{\partial c_w}{\partial z} \right) - \frac{\partial q_a c_a}{\partial z} - \frac{\partial q c_w}{\partial z} - S c_w + P \quad (23)$$

$$P = \gamma_s + \gamma_p$$

where c_w , c_a = volumetric concentrations of CO₂ in the dissolved and gas phases [L³L⁻³], respectively; D_a = effective soil matrix diffusion coefficient of CO₂ in the gas phase [L²T⁻¹]; D_w = effective soil matrix dispersion coefficient of CO₂ in the dissolved phase [L²T⁻¹]; q_a = soil air flux [LT⁻¹]; q = soil water flux [LT⁻¹]; $S c_w$ = dissolved CO₂ removed from the soil by root water uptake [L³L⁻³T⁻¹]; P = CO₂ production/sink term [L³L⁻³T⁻¹]; and γ_s , γ_p = CO₂ production rates by soil microorganisms or plant roots [L³L⁻²T⁻¹], respectively (Šimůnek and Suarez, 1993).

The major variables of the UNSATCHEM chemical system are Ca, Mg, Na, K, SO₄, Cl, NO₃, H₄SiO₄, alkalinity, and CO₂. The model accounts for equilibrium chemical reactions between these components such as complexation, cation exchange and precipitation-dissolution, e.g.,

$$\begin{aligned}
 K_{\text{CaCO}_3} &= \frac{(\text{Ca}^{2+})(\text{CO}_3^{2-})}{(\text{CaCO}_3^0)} \\
 K_{\text{Mg,Ca}} &= \frac{\overline{\text{Mg}}^{2+}}{\overline{\text{Ca}}^{2+}} \frac{(\text{Ca}^{2+})^{1/2}}{(\text{Mg}^{2+})^{1/2}} \\
 K_{\text{SP}}^C &= (\text{Ca}^{2+})(\text{CO}_3^{2-})
 \end{aligned}
 \tag{24}$$

respectively, where the parentheses denote ion activities, K_{CaCO_3} = equilibrium constant of the CaCO_3^0 complexed species [-]; $K_{\text{Mg,Ca}}$ = Gapon selectivity coefficient for Mg^{2+} and Ca^{2+} [-]; and K_{SP}^C = calcite solubility product [-]. Similar algebraic equations hold for all species of the chemical system.

For the precipitation-dissolution of calcite (CaCO_3) and the dissolution of dolomite ($\text{MgCO}_3 \cdot 3\text{H}_2\text{O}$), either equilibrium or multicomponent kinetic expressions can be used, including both forward and backward reactions. Other precipitation-dissolution reactions considered in the UNSATCHEM models involve gypsum ($\text{CaSO}_4 \cdot 2\text{H}_2\text{O}$), hydromagnesite ($\text{Mg}_5(\text{CO}_3)_4(\text{OH})_2 \cdot 4\text{H}_2\text{O}$), nesquehonite ($\text{MgCO}_3 \cdot 3\text{H}_2\text{O}$), and sepiolite ($\text{Mg}_2\text{Si}_3\text{O}_7 \cdot 5(\text{OH}) \cdot 3\text{H}_2\text{O}$). Since the ionic strength of soil solutions can vary considerably in time and space and often reach high values, both the modified Debye-Hückel (Truesdell & Jones 1974) and Pitzer (Pitzer 1979) expressions were incorporated into the model, thus providing options for calculating single-ion activities. The module also considers the effects of solution composition on the unsaturated soil hydraulic properties. The new UNSATCHEM module of HYDRUS-1D enables quantitative predictions of processes involving major ions, such as simulations of the effects of salinity on root water uptake and plant growth, evaluation of alternative irrigation, salinity and crop management practices, evaluation of water suitability for irrigation, and estimation of the amount of water and amendment required to reclaim soil profiles to desired levels of salinity and ESP (exchangeable sodium percentage).

A recent application of HYDRUS-1D and its major ion chemistry module is given by Gonçalves et al. (2005) who simulated solute transport in three lysimeters irrigated with different quality waters over a time period of three years. HYDRUS-1D successfully described field measurements of not only the overall salinity, but also of individual soluble cations as well as SAR (Sodium Adsorption Ratio) (Fig. 5) and ESP (Gonçalves et al. 2005).

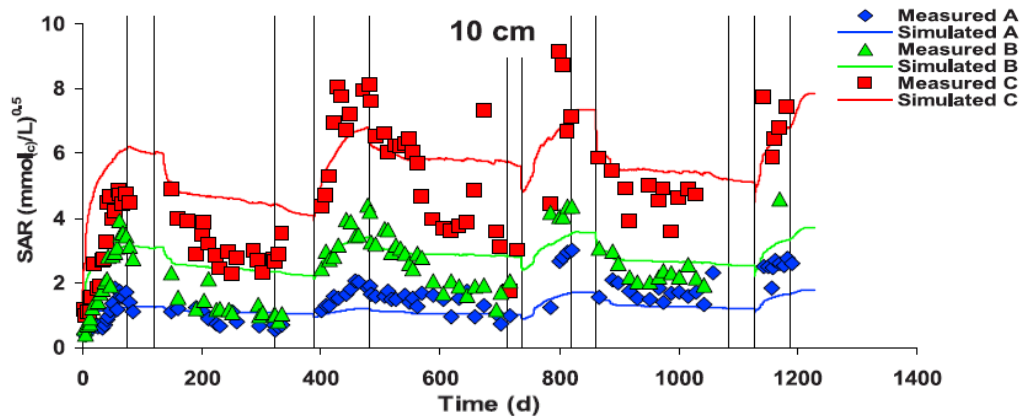


Figure 5. Measured and simulated sodium adsorption ratios (SAR) for lysimeters A, B, and C (Gonçalves et al. 2005).

4.2.2 Chemical and biological reactions in HP1

HYDRUS-1D was recently coupled also with the PHREEQC geochemical code (Parkhurst & Appelo 1999) to create a new comprehensive simulation tool, HP1 (acronym for HYDRUS1D-PHREEQC) (Jacques & Šimůnek 2005; Jacques et al. 2006; Šimůnek et al. 2006a). This new code contains modules simulating (1) transient water flow in variably-saturated media, (2) the transport of multiple components, (3) mixed equilibrium/kinetic biogeochemical reactions, and (4) heat transport. HP1 is a significant expansion of the individual HYDRUS-1D and PHRE-

EQC programs by preserving most of their original features. The code still uses the Richards equation for simulating variably-saturated water flow and advection-dispersion type equations for heat and solute transport. However, the loosely coupled program can simulate also a broad range of low-temperature biogeochemical reactions in water, the vadose zone and in ground water systems, including interactions with minerals, gases, exchangers and sorption surfaces based on thermodynamic equilibrium, kinetic, or mixed equilibrium-kinetic reactions. HP1 uses the operator-splitting approach with no iterations during one time step (a non-iterative sequential modeling approach). Jacques et al. (2006) evaluated the accuracy of the operator-splitting approach for a kinetic reaction network (i.e., sequential and parallel kinetic degradation reactions) by comparing HP1 with an analytical solution for TCE-degradation, as well as for mixed equilibrium and kinetic reactions involving different flow conditions (steady-state and transient).

Jacques & Šimůnek (2005), and Šimůnek et al. (2006a) and Jacques et al. (2006; in press), demonstrated the versatility of HP1 on several examples, which included a) the transport of heavy metals (Zn^{2+} , Pb^{2+} , and Cd^{2+}) subject to multiple cation exchange reactions, b) transport with mineral dissolution of amorphous SiO_2 and gibbsite ($Al(OH)_3$), c) heavy metal transport in a medium with a pH-dependent cation exchange complex, d) infiltration of a hyperalkaline solution in a clay sample (this example considers kinetic precipitation-dissolution of kaolinite, illite, quartz, calcite, dolomite, gypsum, hydrotalcite, and sepiolite), e) long-term transient flow and transport of major cations (Na^+ , K^+ , Ca^{2+} , and Mg^{2+}) and heavy metals (Cd^{2+} , Zn^{2+} , and Pb^{2+}) in a soil profile, f) cadmium leaching in acid sandy soils, g) radionuclide transport, and h) long term uranium migration in agricultural field soils following mineral P-fertilization.

4.2.3 Wetland module

A multi-component reactive transport model CW2D (**Constructed Wetlands 2D**) (Langergraber & Šimůnek 2005, 2006) was developed to model the biochemical transformation and degradation processes in subsurface-flow constructed wetlands. The model was incorporated into the HYDRUS (2D/3D) variably-saturated water flow and solute transport software package. Constructed wetlands have become increasingly popular for removing organic matter, nutrients, trace elements, pathogens, or other pollutants from wastewater and/or runoff water. Such wetlands involve a complex mixture of water, substrate, plants, litter, and a variety of microorganisms to provide optimal conditions for improving water quality. The water flow regime in subsurface-flow constructed wetlands can be highly dynamic and requires the use of transient variably-saturated flow model. The biochemical components defined in CW2D include dissolved oxygen, three fractions of organic matter (readily- and slowly-biodegradable, and inert), four nitrogen compounds (ammonium, nitrite, nitrate, and dinitrogen), inorganic phosphorus, and heterotrophic and autotrophic micro-organisms. Organic nitrogen and organic phosphorus were modeled as part of the organic matter. The biochemical degradation and transformation processes were based on Monod-type rate expressions, such as for NO_3 -based growth of heterotrophs on readily biodegradable COD (denitrification):

$$r = \mu_{DN} \frac{K_{DN,O_2}}{K_{DN,O_2} + c_{O_2}} \frac{c_{NO_3}}{K_{DN,NO_3} + c_{NO_3}} \frac{K_{DN,NO_2}}{K_{DN,NO_2} + c_{NO_2}} \frac{c_{CR}}{K_{DN,CR} + c_{CR}} f_{N,DN} c_{XH} \quad (25)$$

We refer to Langergraber & Šimůnek (2005, 2006) for a detailed discussion of the terms in (25). All process rates and diffusion coefficients were assumed to be temperature dependent. Heterotrophic bacteria were assumed to be responsible for hydrolysis, mineralization of organic matter (aerobic growth) and denitrification (anoxic growth), while autotrophic bacteria were assumed to be responsible for nitrification, which was modeled as a two-step process. Lysis was considered to be the sum of all decay and sink processes. Langergraber & Šimůnek (2005, 2006) demonstrated the model for one- and two-stage subsurface vertical flow constructed wetlands. Model simulations of water flow, tracer transport, and selected biochemical compounds were compared against experimental observations.

5 NUMERICAL SOLUTIONS

All models discussed in this manuscript are numerical models that use various techniques to solve the governing partial differential equations. While spatial derivatives are invariably approximated using the Galerkin-type linear finite element schemes, temporal derivatives in the models are approximated using finite differences. We always used a fully implicit (backward) finite difference scheme for water flow, and a Crank-Nicholson time-centered scheme for heat and solute transport. The mass-conservative method proposed by Celia et al. (1990) was used in all HYDRUS models. This method has been shown to provide excellent results in terms of minimizing the mass balance error. Time and space discretization of the Richards equation generally leads to a nonlinear system of algebraic equations. These equations are then linearized and solved using the Picard iteration method. Higher-order approximations for the time derivative as derived by van Genuchten (1976) are used for discretization of the transport equations. Depending upon the size of the problem, the matrix equations resulting from discretization of the governing equations are solved using either Gaussian elimination for banded matrices, or the conjugate gradient method for symmetric matrices and the ORTHOMIN method for asymmetric matrices (Mendoza et al. 1991).

The operator-splitting approach with no iterations during one time step (non-iterative sequential approach) is used in all multicomponent models (i.e., for the major ion chemistry module of HYDRUS-1D, in HP1, and in the wetland CW2D module of HYDRUS (2D/3D)).

Three-dimensional applications in general require a large number of finite elements to discretize realistically large transport domains. Even with the fast personal computers currently available, it is still very difficult to solve within a reasonable time problems having more than about half million nodes. To decrease the required computational time, Hardelauf et al. (2007) parallelized SWMS_3D to develop PARSWMS that distributes problems with a large number of elements over multiple processors working in parallel. The PARSWMS code was developed for the LINUX or UNIX workstations with installed free-ware MPI, PETSc and PARMETIS. Hardelauf et al. (2007) demonstrated that doubling the number of processors may lead to a decrease in the computational time of up to 48 %.

6 GRAPHICAL USER INTERFACES

One major problem often preventing the use of numerical codes is the extensive work required for data preparation, finite element grid design, and graphical presentation of the output results. Hence, a more widespread use of numerical models requires techniques which make it easier to create, manipulate and display large data files, and which facilitate interactive data management (Šimůnek et al. 1999). Introducing such techniques frees users from cumbersome manual data processing, and enhances the efficiency in which programs are being implemented for a particular example. To avoid or simplify the preparation and management of relatively complex input data files and to graphically display final simulation results, we were very keen in developing interactive graphics-based user-friendly interfaces (GUIs) for the MS Windows environments. From 1995 on this has resulted into several of the software packages described above. While earlier versions (until 1998) were still 16-bit applications, all software packages from 1998 on are 32-bit applications fully compatible with all Windows operating systems released after Windows 95.

7 CONCLUSIONS

Over the last 15 years the close collaboration between the University of California Riverside, and the U.S. Salinity Laboratory, and more recently with PC-Progress in Prague, Czech Republic, and SCK•CEN, Mol, Belgium, resulted in the development of a large number of computer tools that are currently being used worldwide for a variety of applications involving the vadose zone. The numerical models may be used to simulate not only one- and multi-dimensional water flow, heat transport and solute transport in variably saturated media, but also the transport of carbon dioxide, major ions, trace elements, colloids, viruses, bacteria, and wastewater. The popularity of the modeling tools is in large part due to their ease of use because of the availabil-

ity of interactive graphical user interfaces. While the earlier models have proved to be useful for analyzing subsurface flow and processes, several more complex models and modules are being developed at present. One example is the HP1 code that couples the HYDRUS-1D water flow and solute transport model with the PHREEQC geochemical model. Since the resulting combined program brings together the state-of-the-art in both flow and transport modeling and modeling of geochemical reactions, we believe that HP1 represents a very flexible and promising tool for evaluating complex interactions of various processes in the vadose zone.

ACKNOWLEDGEMENT

This paper is based on work supported in part by the Terrestrial Sciences Program of the Army Research Office (Terrestrial Processes and Landscape Dynamics and Terrestrial System Modeling and Model Integration), by the National Science Foundation Biocomplexity programs #04-10055 and NSF DEB 04-21530, and by SAHRA (Sustainability of semi-Arid Hydrology and Riparian Areas) under the STC Program of the National Science Foundation, Agreement No. EAR-9876800.

REFERENCES

- Appelo, C. A. J. & Postma, D. 2005. *Geochemistry, Groundwater and Pollution*, 2nd ed., A. A. Balkema Publ., Leiden, The Netherlands, 649 p.
- Bradford, S. A., Bettahar, M., Šimůnek, J. & van Genuchten, M. Th. 2004. Straining and attachment of colloids in physically heterogeneous porous media. *Vadose Zone J.* 3(2), 384-394.
- Bradford, S. A., Šimůnek, J., Bettahar, M., van Genuchten, M. Th. & Yates, S. R. 2006. Significance of straining in colloid deposition: evidence and implications. *Water Resour. Res.*, 42, W12S15, doi:10.1029/2005WR004791, 16 pp.
- Brooks, R. H. & Corey, A. T. 1964. Hydraulic properties of porous media. *Hydrol. Paper No. 3*, Colorado State Univ., Fort Collins, CO.
- Casey, F. X. M. & Šimůnek, J. 2001. Inverse analyses of the transport of chlorinated hydrocarbons subject to sequential transformation reactions. *J. of Environ. Quality*, 30(4), 1354-1360.
- Casey, F. X. M., Larsen, G. L., Hakk, H. & Šimůnek, J. 2003. Fate and transport of 17 β -Estradiol in soil-water systems. *Environ. Sci. Technol.*, 37(11), 2400-2409.
- Castiglione, P., Mohanty, B. P., Shouse, P. J., Šimůnek, J., van Genuchten, M. Th., & Santini, A. 2003. Lateral water diffusion in an artificial macroporous system: Theory and experimental evidence. *Vadose Zone J.*, 2, 212-221.
- Celia, M. A., Bououtas, E. T. & Zarba, R. L. 1990. A general mass-conservative numerical solution for the unsaturated flow equation. *Water Resour. Res.*, 26, 1483-1496.
- de Vries, D. A. 1958. Simultaneous transfer of heat and moisture in porous media. *Transactions, American Geophysical Union*, 39(5), 909-916.
- Dontsova, K. M., Yost, S. L., Šimůnek, J., Pennington, J. C. & Williford, C. 2006. Dissolution and transport of TNT, RDX, and Composition B in saturated soil columns. *J. of Environ. Quality*, 35, 2043-2054.
- Durner, W. 1994. Hydraulic conductivity estimation for soils with heterogeneous pore structure. *Water Resour. Res.*, 32(9), 211-223.
- Gargiulo, G., Bradford, S. A., Šimůnek, J., Ustohal, P., Vereecken, H. & Klumpp, E. 2007. Transport and deposition of metabolically active and stationary phase *Deinococcus Radiodurans* in unsaturated porous media. *Environ. Sci. and Technol.*, 41(4), 1265-1271.
- Gerke, H. H., & van Genuchten, M. Th., 1993. A dual-porosity model for simulating the preferential movement of water and solutes in structured porous media. *Water Resour. Res.* 29, 305-319.
- Gonçalves, M. C., Šimůnek, J., Ramos, T. B., Martins, J. C., Neves, M. J. & Pires, F. P. 2006. Multicomponent solute transport in soil lysimeters irrigated with waters of different quality. *Water Resour. Res.*, 42, W08401, doi:10.1029/2006WR004802, 17 pp.
- Hanson, B. R., Šimůnek, J. & Hopmans, J. W. 2006. Numerical modeling of urea-ammonium-nitrate fertigation under microirrigation. *Agric. Water Management*, 86, 102-113.
- Hansson, K., Šimůnek, J., Mizoguchi, M., & Lundin, L.-Ch. 2004. Water flow and heat transport in frozen soil: Numerical solution and freeze/thaw applications. *Vadose Zone Journal*, 3(2), 693-704.

- Harbaugh, A.W., Banta, E. R., Hill, M. C. & McDonald, M. G. 2000. MODFLOW-2000, the U.S. Geological Survey modular ground-water model user guide to modularization concepts and the ground-water flow process. Denver, CO, Reston, VA, U.S. Geological Survey.
- Hardelauf, H., Javaux, M., Herbst, M., Gottschalk, S., Kasteel, R., Vanderborght, J. & Vereecken, H. 2007. PARSWMS: a parallelized model for simulating 3-D water flow and solute transport in variably saturated soils. *Vadose Zone Journal*, 6(2), 255-259.
- Haws, N. W., Rao, P. S. C., Šimůnek, J. & Poyer I. C. 2005. Single-porosity and dual-porosity modeling of water flow and solute transport in subsurface-drained fields using effective field-scale parameters. *J. of Hydrology*, 313(3-4), 257-273.
- Hendrickx, J. M. H., Dekker, L. W., & Boersma, O. H. 1993. Unstable wetting fronts in water repellent field soils. *J. Environ. Qual.* 22, 109-118.
- Jacques, D. & Šimůnek, J. 2005. User Manual of the Multicomponent Variably-Saturated Flow and Transport Model HPI, Description, Verification and Examples. Version 1.0, *SCK•CEN-BLG-998*, Waste and Disposal, SCK•CEN, Mol, Belgium, 79 pp.
- Jacques, D., Šimůnek, J., Mallants, D. & van Genuchten, M. Th. 2006. Operator-splitting errors in coupled reactive transport codes for transient variably saturated flow and contaminant transport in layered soil profiles. *J. Contam. Hydrology*, 88, 197-218.
- Jacques, D., Šimůnek, J., Mallants, D. & van Genuchten, M. Th. 2008. Modeling coupled hydrological and chemical processes in the vadose zone: a case study on long term uranium migration following mineral p-fertilization, *Vadose Zone J.*, Special Issue “Vadose Zone Modeling”, (in press).
- Kodešová, R., Kozák, J., Šimůnek, J. & Vacek, O. 2005. Field and numerical study of chlorotoluron transport in the soil profile: Comparison of single and dual-permeability model. *Plant, Soil and Environment*, 51(7), 310-315.
- Köhne, J. M., Köhne, S., Mohanty, B. P. & Šimůnek, J. 2004. Inverse mobile-immobile modeling of transport during transient flow: Effect of between-domain transfer and initial water content. *Vadose Zone J.*, 3(4), 1309-1321
- Köhne, J. M. & Mohanty, B. P. 2005. Water flow processes in a soil column with a cylindrical macropore: Experiment and hierarchical modeling. *Water Resour. Res.*, 41, W03010, doi:10.1029/2004WR003303.
- Köhne, J. M., Mohanty, B. P. & Šimůnek, J. 2006. Inverse dual-permeability modeling of preferential water flow in a soil column and implications on field-scale solute transport prediction. *Vadose Zone Journal*, 5, 59-76.
- Kosugi K. 1996. Lognormal distribution model for unsaturated soil hydraulic properties. *Water Resour. Res.*, 32(9), 2697-2703.
- Kung, K-J. S. 1990. Preferential flow in a sandy vadose zone. 2. Mechanism and implications. *Geoderma*, 46, 59-71.
- Langergraber, G. & Šimůnek, J. 2005. Modeling Variably-Saturated Water Flow and Multi-Component Reactive Transport in Constructed Wetlands. *Vadose Zone Journal*, 4, 924-938.
- Langergraber, G. & Šimůnek, J. 2006. The Multi-component Reactive Transport Module CW2D for Constructed Wetlands for the HYDRUS Software Package, Manual – Version 1.0, *HYDRUS Software Series 2*, Department of Environmental Sciences, University of California Riverside, Riverside, CA, 72 pp.
- Mendoza, C. A., Therrien, R. & Sudicky, E. A. 1991. *ORTHOPEM User's Guide, Version 1.02*. Waterloo Centre for Groundwater Research, Univ. of Waterloo, Waterloo, Ontario, Canada.
- Parkhurst, D. L. & Appelo, C. A. J. 1999. User's guide to PHREEQC (version 2) – A computer program for speciation, batch-reaction, one-dimensional transport, and inverse geochemical calculations. Water Resources Investigation, Report 99-4259, Denver, Co, USA, 312 pp.
- Pitzer, K. S. 1979. *Activity Coefficients in Electrolyte Solutions*. Chap. 7, CRC Press, Boca Raton, FL.
- Pot, V., Šimůnek, J., Benoit, P., Coquet, Y., Yra, A. & Martínez-Cordón, M.-J. 2005. Impact of rainfall intensity on the transport of two herbicides in undisturbed grassed filter strip soil cores. *J. of Contaminant Hydrology*, 81, 63-88.
- Saito, H., J., Šimůnek, J. & Mohanty, B. 2006. Numerical analyses of coupled water, vapor and heat transport in the vadose zone. *Vadose Zone Journal*, 5, 784–800.
- Scanlon, B., Keese, K., Reedy, R. C., Šimůnek, J. & Andraski, B. 2003. Variations in flow and transport in thick desert vadose zones in response to paleoclimatic forcing (0 – 90 kyr): Monitoring, modeling, and uncertainties. *Water Resour. Res.* 39(7), 1179, doi:10.1029/2002WR001604, 13.1-13.7.
- Schaerlaekens, J., Mallants, D., Šimůnek, J., van Genuchten, M. Th. & Feyen, J. 1999. Numerical simulation of transport and sequential biodegradation of chlorinated aliphatic hydrocarbons using CHAIN_2D. *J. of Hydrological Processes*, 13(17), 2847-2859.
- Šejna, M. & Šimůnek, J. 2007. HYDRUS (2D/3D): Graphical User Interface for the HYDRUS Software Package Simulating Two- and Three-Dimensional Movement of Water, Heat, and Multiple Solutes in Variably-Saturated Media, published online at www.-pc-progress.cz, PC-Progress, Prague, Czech Republic.

- Seo, H. S., Šimůnek, J. & Poeter, E. P. 2006. Application of the Unsaturated Flow (UNSF) Package, Modflow Conference Proceedings, ed. E. Poeter, Ch. Zheng, M. Hill, and J. Doherty, International Ground Water Modeling Center, Colorado School of Mines, May 22-24, Golden, CO.
- Seo, H. S., Šimůnek, J. & Poeter, E. P. 2007. Documentation of the HYDRUS package for MODFLOW-2000, the U.S. Geological Survey Modular Ground-Water Model. *GWMI 2007-01*. International Ground Water Modeling Center, Colorado School of Mines, Golden, Colorado, 96 pp.
- Šimůnek, J. & Suarez, D. L. 1993. Modeling of carbon dioxide transport and production in soil: 1. Model development. *Water Resour. Res.*, 29(2), 487-497.
- Šimůnek, J. & Suarez, D. L. 1994. Two-dimensional transport model for variably saturated porous media with major ion chemistry. *Water Resour. Res.*, 30(4), 1115-1133.
- Šimůnek, J., Vogel, T. & van Genuchten, M. Th. 1994. SWMS_2D simulating water flow and solute transport in two-dimensional variably saturated media. Version 1.2, *IGWMC - FOS 61*, International Ground Water Modeling Center, Colorado School of Mines, Golden, Colorado, 196 pp.
- Šimůnek, J., Huang, K. & van Genuchten, M. Th. 1995. The SWMS_3D code for simulating water flow and solute transport in three-dimensional variably saturated media. Version 1.0, *Research Report No. 139*, U.S. Salinity Laboratory, USDA, ARS, Riverside, California, 155 pp.
- Šimůnek, J., Šejna, M. & van Genuchten, M. Th. 1999. The HYDRUS-2D software package for simulating two-dimensional movement of water, heat, and multiple solutes in variably saturated media. Version 2.0, *IGWMC - TPS - 53*, International Ground Water Modeling Center, Colorado School of Mines, Golden, Colorado, 251 pp.
- Šimůnek, J., Wendroth, O., Wypler, N., & van Genuchten, M. Th. 2001. Nonequilibrium water flow characterized from an upward infiltration experiment. *European J. of Soil Sci.*, 52(1), 13-24.
- Šimůnek, J. & Valocchi, A. J. 2002. Geochemical Transport. In: *Methods of Soil Analysis*, Part 1, Physical Methods. Chapter 6.9, Eds. J. H. Dane and G. C. Topp, Third edition, SSSA, Madison, WI, 1511-1536.
- Šimůnek, J. 2003. *HYDRUS-2D Code Modification: Modeling Overland Flow and Dynamic Interactions Between Plants and Water Flow in a Hillslope Transect*. Idaho National and Environmental Laboratory, Final report for project under contract number 00021013, 55 pp.
- Šimůnek, J., Jarvis, N. J., van Genuchten, M. Th. & Gärdenäs, A. 2003. Nonequilibrium and preferential flow and transport in the vadose zone; review and case study. *Journal of Hydrology*, 272, 14-35.
- Šimůnek, J., van Genuchten, M. Th. & Šejna, M. 2005. The HYDRUS-1D software package for simulating the one-dimensional movement of water, heat, and multiple solutes in variably-saturated media. Version 3.0, *HYDRUS Software Series 1*, Department of Environmental Sciences, University of California Riverside, Riverside, CA, 270 pp.
- Šimůnek, J., Jacques, D., van Genuchten, M. Th. & Mallants, D. 2006a. Multicomponent geochemical transport modeling using the HYDRUS computer software packages. *J. Am. Water Resour. Assoc.*, 42(6), 1537-1547.
- Šimůnek, J., van Genuchten, M. Th. & Šejna, M. 2006b. *The HYDRUS Software Package for Simulating Two- and Three-Dimensional Movement of Water, Heat, and Multiple Solutes in Variably-Saturated Media*. Technical Manual, Version 1.0, PC Progress, Prague, Czech Republic, pp. 241.
- Šimůnek, J. & van Genuchten, M. Th. 2008. Modeling nonequilibrium flow and transport with HYDRUS. *Vadose Zone Journal*, Special Issue “Vadose Zone Modeling”, (in press).
- Šimůnek, J., van Genuchten, M. Th. & Šejna, M. 2008. Development and applications of HYDRUS and related software packages. *Vadose Zone Journal*, Special Issue “Vadose Zone Modeling”, (in press).
- Truesdell, A. H. & Jones, B. F. 1974. WATEQ, a computer program for calculating chemical equilibria of natural waters. *J. Res. U. S. Geol. Surv.*, 2(2), 233-248.
- Twarakavi, N. K. C., Šimůnek, J. & Seo, H. S. 2008. Evaluating interactions between groundwater and vadose zone using HYDRUS-based flow package for MODFLOW, *Vadose Zone J.*, Special Issue “Vadose Zone Modeling”, (in press).
- van Genuchten, M. Th. 1976. On the accuracy and efficiency of several numerical schemes for solving the convective-dispersive equation, in *Finite Elements in Water Resources*, edited by W. G. Gray et al., Pentech Press, London, pp. 1.71-1.90.
- van Genuchten, M. Th. & Wierenga, P. J. 1976. Mass transfer studies in sorbing porous media, I. Analytical solutions. *Soil Sci. Soc. Am. J.* 40, 473-481.
- van Genuchten, M. Th. 1980. A closed-form equation for predicting the hydraulic conductivity of unsaturated soils. *Soil Sci. Soc. Am. J.*, 44, 892-898.
- Wang, D., Yates, S. R. & Gan, J. 1997. Temperature effect on methyl bromide volatilization in soil fumigation. *Journal of Environmental Quality*, 26(4), 1072-1079.
- Wang, D., Knuteson, J. A. & Yates, S. R. 2000. Two-dimensional model simulation of 1,3-dichloropropene volatilization and transport in a field soil. *Journal of Environmental Quality*, 29(2), 639-644.

Zhang, P., Šimůnek, J., & Bowman, R. S. 2004. Nonideal transport of solute and colloidal tracers through reactive zeolite/iron pellets. *Water Resour. Res.*, 40, doi:10.1029/2003WR002445.

OUTLINE:

1. Introduction
2. Water Flow
 - 2.1. Uniform Flow
 - 2.2. Nonequilibrium Flow
 - 2.3. Water Flow and Vapor Transport
 - 2.4. Water Flow with Freezing and Thawing
 - 2.5. Overland Flow
 - 2.6. HYDRUS package for MODFLOW
3. Heat Transport
 - 3.1. Heat Transport without Vapor Transport
 - 3.2. Heat Transport with Vapor Transport
 - 3.3. Heat Transport with Freezing and Thawing
4. Solute Transport
 - 4.1. Single Component Solute Transport
 - 4.1.1. Equilibrium Transport
 - 4.1.2. Nonequilibrium Transport
 - 4.2. Multicomponent Solute Transport
 - 4.2.1. Major Ion Chemistry
 - 4.2.2. Chemical and Biological Reactions in HP1
 - 4.2.3. Wetland Module
5. Numerical Solutions
6. Graphical Interfaces
7. Summary and Conclusions